

ON THE ORIGIN OF THE SOLAR MESOGRANULATION

FAUSTO CATTANEO

Department of Mathematics, University of Chicago, 5734 South University Avenue, Chicago, IL 60637; cattaneo@math.uchicago.edu

DAWN LENZ¹

Department of Astronomy and Astrophysics, University of Chicago, 5640 South Ellis Avenue, Chicago, IL 60637; lenz@oddjob.uchicago.edu

AND

NIGEL WEISS

Department of Applied Mathematics and Theoretical Physics, University of Cambridge, Cambridge CB3 9EW, UK; n.o.weiss@damtp.cam.ac.uk

Received 2001 March 13; accepted 2001 October 30; published 2001 November 26

ABSTRACT

The observed properties of mesogranules are related to structures found in idealized numerical experiments on turbulent convection. We describe results obtained for three-dimensional Boussinesq convection in a layer with a very large aspect ratio. There are two distinct cellular patterns at the surface. Energy-transporting convection cells (corresponding to granules in the solar photosphere) have diameters comparable to the layer depth, while macrocells (corresponding to mesogranules) are several times larger. The motion acts as a small-scale turbulent dynamo, generating a disordered magnetic field that is concentrated at macrocellular corners and, to a lesser extent, in the lanes that join them. These results imply that mesogranules owe their origin to collective interactions between the granules.

Subject headings: Sun: granulation — Sun: magnetic fields — Sun: photosphere

1. INTRODUCTION

Observations reveal three different cellular patterns on the surface of the Sun. Two patterns have been studied for many years (Bray, Loughhead, & Durrant 1984): granules, with a characteristic diameter of 1400 km, are responsible for energy transport and are now being observed with extraordinary precision from the ground (e.g., Berger et al. 1998), while supergranules, which are outlined by the photospheric network and have typical diameters of 20,000–30,000 km, can be tracked for long periods from space (e.g., Duvall & Gizon 2000; Shine, Simon, & Hurlburt 2000). Mesogranules, with diameters on the order of 6000 km, were first identified by November et al. (1981); more recently, they have been followed continuously for 3 hr at the Pic du Midi (Muller et al. 1992) and for 45 hr with the Michelson Doppler Instrument on board the *Solar and Heliospheric Observatory* from space (Shine et al. 2000). These observations have confirmed that mesogranules are real features; correlation tracking shows that individual granules are transported outward to mesogranular boundaries where magnetic fields accumulate, as predicted by the behavior of test particles (or “corks”). Moreover, the mesogranules themselves move with the supergranular flow toward the network at supergranule boundaries, where they are destroyed. Helioseismic measurements indicate that the supergranules are at least 8000 km deep (Kosovichev, Duvall, & Scherrer 2000), while accurate power spectra reveal a clear gap between supergranules and smaller scale structures (Hathaway et al. 2000). Although any distinction between mesogranules and granules is smeared out in ordinary power spectra, a recent wavelet analysis has confirmed the presence of two different scales (Lawrence, Cadavid, & Ruzmaikin 2001). These results demonstrate that there are indeed three distinct convective scales at the photosphere.

Supergranules and granules apparently correspond to separate cellular scales in a strongly stratified atmosphere, possibly related to the levels where He and H are ionized. There have been several speculative attempts to explain the origin of mesogranules. Stein & Nordlund (1989, 1998) have suggested that they are caused

by the progressive amalgamation of sinking plumes in a compressible atmosphere (Spruit, Nordlund, & Title 1990). Mesogranules are also associated with exploding granules, whose splitting is preceded by the formation of a dark core due to buoyancy braking, an effect that again relies on compressibility of the gas (Spruit et al. 1990). Indeed, it has been claimed that the mesogranular pattern simply reflects the presence of families of successively fragmenting granules, as suggested by a two-dimensional simulation of photospheric convection (Ploner, Solanki, & Gadun 2000). However, a careful comparison of kinematic models of photospheric convection with the structures observed by Muller et al. (1992) indicated that while exploding granules do have a significant effect, there is still a separate mesogranular flow (Simon, Title, & Weiss 1991).

In this Letter we exploit the similarity between mesogranules and patterns found in numerical experiments on turbulent convection. In our model calculations we find that small-scale convection cells (corresponding to granules) are spatially modulated on a somewhat larger scale, giving rise to a macrocellular pattern (corresponding to mesogranules) in the convecting layer. The macrocells show up in the horizontal velocity at the surface, in the magnetic field and vorticity patterns, and in the motion of corks. The resemblance between these structures and mesogranules suggests that they have a common origin.

Our numerical experiments on convection in a very wide box (with dimensions $20 \times 20 \times 1$, requiring $1024 \times 1024 \times 96$ mesh points) arose out of a study of small-scale turbulent dynamo action (Cattaneo 1999). The advantage of adopting the Boussinesq approximation is that it allows us to reach exceptionally high values of the Rayleigh number ($R = 5 \times 10^5$) in these calculations, so convection is extremely vigorous. The magnetic diffusivity is kept small compared with the either thermal or viscous diffusivities.

Since the fluid is incompressible, the macrocellular pattern can have nothing to do with stratification. There is no opportunity for sinking plumes to amalgamate, there is no buoyancy braking and no ionization, nor are there any exploding granules. Hence we conclude that the macrocells can be caused only by collective

¹ Present address: Research Systems, Inc., 4990 Pearl East Circle, Boulder, CO 80301.

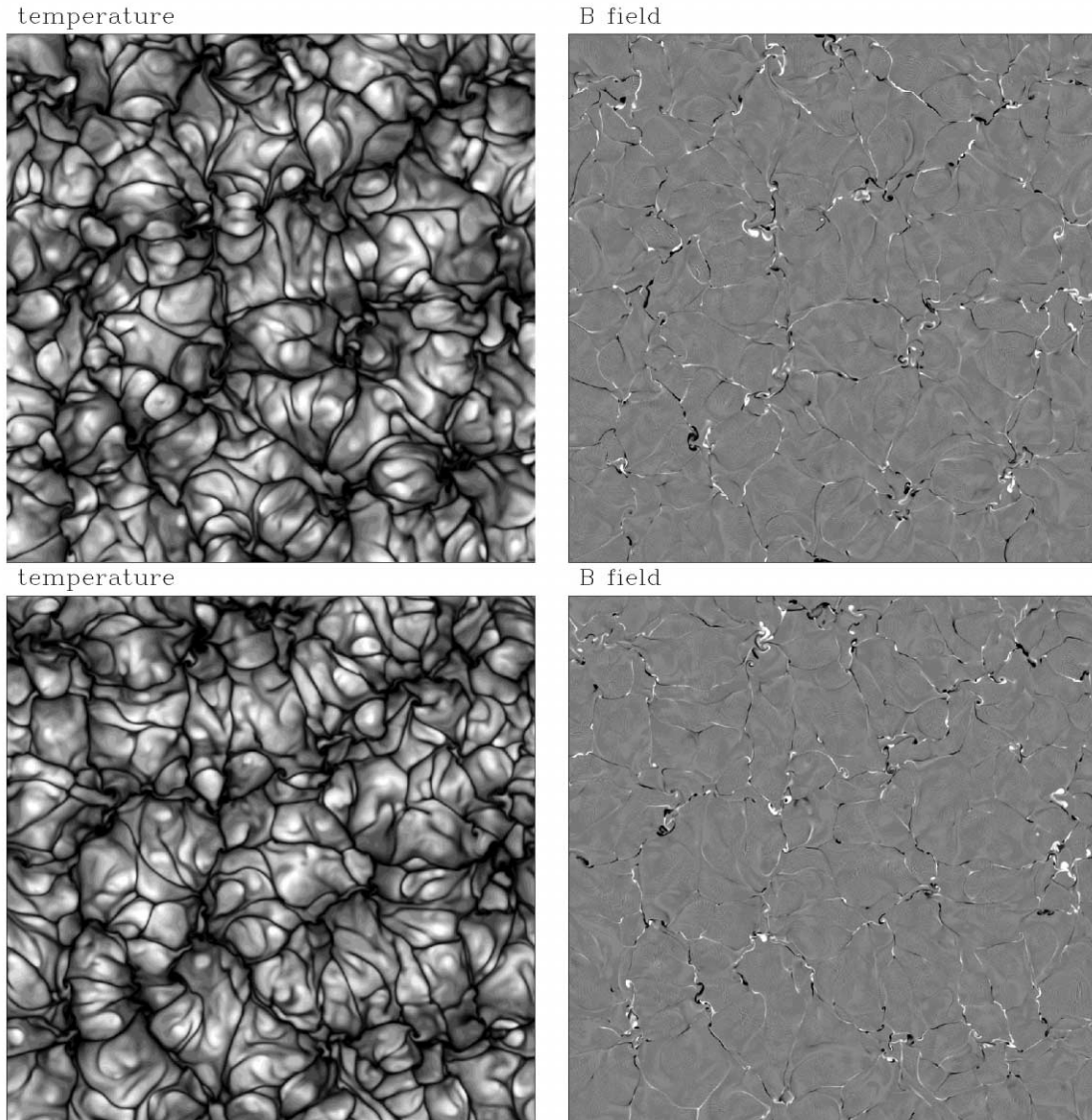


FIG. 1.—Temperature fluctuations and vertical component of the magnetic field in a horizontal plane approximately 1% of the layer depth away from the upper surface. In the left panels (temperature plots), light tones correspond to hot fluid and dark tones to cold fluid; in the right panels (magnetic field), light and dark tones correspond to the two polarities of magnetic field. The two sets of panels are 0.0193 dimensionless time units apart, corresponding approximately to two turnover times. These patterns are characteristic of the thermal boundary layers; in the present calculations they extend for approximately 10% of the depth of the layer.

interactions among the smaller convection cells, and we propose, by analogy, that mesogranules have a similar explanation.

The model problem is described in § 2, and our results are presented in § 3, where we discuss both the smaller convection cells and the larger macrocellular pattern, as revealed by magnetic fields, sources of outflow, and cork motions. Then, in § 4 we consider the physical mechanisms that are responsible for the macroscale pattern, focusing on the role of vorticity. Our numerical results are much easier to interpret when time-dependent behavior can be visualized through movies.²

2. FORMULATION OF THE MODEL

The formulation is essentially that of Cattaneo (1999). We consider fully three-dimensional convection in a horizontal layer of incompressible (Boussinesq) fluid with constant viscosity and thermal diffusivity. The fluid has finite electrical

conductivity, and we allow for the spontaneous generation of magnetic fields, i.e., dynamo action. The layer is bounded above and below by impenetrable, stress-free boundaries on which the temperature is kept constant and the horizontal components of the magnetic field vanish. The solutions are assumed to be periodic in the two horizontal directions.

For the computations described herein, the Rayleigh number is $R = 500,000$, roughly 760 times the critical value for the onset of convection. The kinetic and magnetic Prandtl numbers are 1 and 5, respectively. The computational domain is 20 times wider in each horizontal direction than it is deep. For a typical simulation, a state of vigorous convection develops from random initial conditions in a few turnover times. This nonlinear convective state is an efficient small-scale dynamo that leads to the generation of a random magnetic field in a few more turnover times. The resulting statistically stationary state then persists for as long as the computation is continued.

The present work is based on two related sets of numerical solutions with aspect ratios $10 \times 10 \times 1$ and $20 \times 20 \times 1$. The

² A selection of relevant MPEG movies can be inspected on the Web site at <http://flash.uchicago.edu/mhd>.

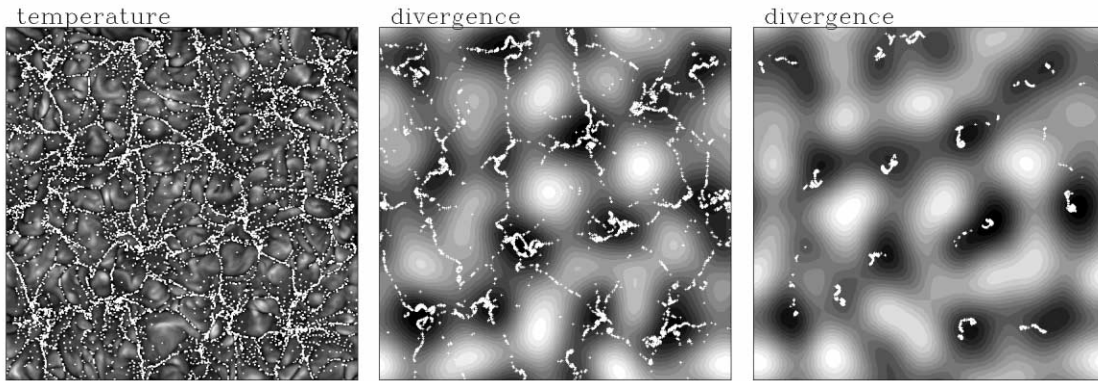


FIG. 2.—Time evolution of passive tracers (corks). The three panels show the distribution of passive tracers at three selected times $t = 0.0023$, $t = 0.008$, and $t = 0.057$, corresponding physically to one-fifth, four-fifths, and six turnover times. Initially, the 10,000 corks are distributed uniformly. In the left panel the temperature distribution is superposed on the corks. In the middle and right panels the coarse-grained (horizontal) divergence Δ is shown; light and dark tones correspond to regions of divergence and convergence, respectively. The coarse graining was effected by convolving the horizontal velocity with a Gaussian filter of width 2.

solution with the smaller aspect ratio was started from random initial conditions, evolved to a stationary state with a fully developed dynamo magnetic field, and then continued for over 150 turnover times.³ The solution with aspect ratio $20 \times 20 \times 1$ was obtained by placing four copies of the solution with aspect ratio $10 \times 10 \times 1$ side by side. To break the resulting fourfold symmetry, a nonsymmetric temperature perturbation was superposed on this symmetric state, leading after a few turnovers to a nonsymmetric solution. After the initial symmetry was lost the computation was continued for over 35 turnover times. Many of the properties discussed in the present work are already apparent in the simulations with smaller aspect ratio. The simulations with larger aspect ratio were carried out to ensure that the observed effects were not an artifact of a too restrictive geometry. All the discussions presented in this Letter pertain to properties of the solutions in a statistically stationary state.

3. RESULTS

In this section we describe the statistically steady state of convection characterized by a Reynolds number of 200 and a magnetic Reynolds number of 1000, based on the rms velocity and layer depth. In this regime the turbulent motion acts as an efficient small-scale dynamo, generating a highly intermittent magnetic field with no net flux through the layer; the total magnetic energy is 20% of the kinetic energy (Cattaneo 1999).

The temperature plots in Figure 1 show a disordered pattern of cellular convection. The individual cells that are responsible for transporting heat have some internal fine structure but are clearly outlined by prominent dark lanes. Although highly irregular in shape, the cells have a characteristic width of 1–3 times the layer depth. The convection is strongly time dependent: cells are constantly being created and destroyed and their average lifetime is comparable to the turnover time.

The magnetic pattern is utterly different. The most prominent features are isolated field concentrations. These are separated by distances much larger than the width of the convection cells, whose boundaries are barely visible. The field concentrations are linked by a filamentary network that forms a *macrocellular* pattern whose characteristic scale is 2–3 times that of the convection cells. Upon comparing the temperature and magnetic plots it becomes apparent that the field concentrations coincide with particularly dark cool features (which are actually the sites of

strong downflows). Closer scrutiny shows that the filamentary magnetic network likewise coincides with a corresponding macrocellular network of prominent dark lanes in the temperature distribution.

The macrocells evolve on a timescale that is much longer than the lifetime of the convection cells. The flux concentrations, which are located at macrocellular corners, typically persist throughout our experiment. The whole pattern slowly evolves as these corners drift about. This process can be seen by comparing the upper and lower pairs of panels in Figure 1. Despite the changing pattern, the characteristic width of the macrocells remains unaltered and there is no sign of any larger scale, although the 20×20 box provides ample scope for larger structures to appear.

There is a persistent large-scale flow associated with these macrocells. To see this we first obtain the horizontal velocity \mathbf{u}_H at the upper boundary and then filter out the convection cells by Fourier space averaging to obtain a smoothed velocity $\bar{\mathbf{u}}_H$. This consists of outflows from the mesogranular centers toward their boundaries, focused on their corners. The flow is best visualized by computing the divergence $\Delta = \nabla \cdot \bar{\mathbf{u}}_H$, which evolves slowly as shown in Figure 2. To demonstrate the effects of this flow we track the motion of passive test particles (corks) moving with velocity $\mathbf{u}_H(t)$. Figure 2 illustrates the evolution of the cork pattern, starting with corks distributed uniformly across the upper surface. Within one turnover time the corks are swept to the edges of the convection cells; then they move toward the edges and corners of the macrocells and (after 4–5 turnover times) accumulate at their corners. These corners are the sites of strong persistent downflows that move slowly as the macrocellular pattern evolves. The motion of the corks is indicative of the behavior of other advected quantities, including magnetic fields and the vertical component of the vorticity. Furthermore, the individual convection cells are carried away from the macrocellular centers toward the large-scale network, where they are squeezed out of existence. Indeed, the velocity $\bar{\mathbf{u}}_H$ could perfectly well have been constructed by correlation tracking using the proper motions of convection cells.

4. ORIGIN OF MACROSCALE PATTERNS

It is natural to seek a cause for this large-scale motion. Is the magnetic field essential or is it merely a convenient diagnostic? F. Cattaneo, T. Emonet, & N. O. Weiss (2001, in preparation) have obtained a solution for the corresponding *nonmagnetic*

³ We define the turnover time to be *twice* the vertical crossing time based on the root mean square velocity.

problem in a $10 \times 10 \times 1$ box, which is still large enough for macrocells to be recognized (cf. Cattaneo 1999). The dark channels and macroscale divergence pattern are clearly visible in this field-free configuration, so the magnetic fields cannot be responsible for macrocells, which must be a purely hydrodynamic phenomenon.

We can distinguish two aspects of the macrocellular problem. On the one hand, we need to explain the existence of a large-scale convective pattern at any individual instant of time; on the other, we have to identify the mechanism that is responsible for its longevity. The former explanation can readily be given. Strong downflows are a consequence of having an irregular pattern of small-scale cellular convection. Any random distribution of sources and sinks with some characteristic size will lead to some strong downflows on a larger scale, as a purely kinematic effect. This is clearly demonstrated in kinematic modeling of supergranulation (Simon, Title, & Weiss 1995). The strong downflows lead to a large-scale horizontal flow that transports convection cells toward them and is visible in smoothed divergence plots.

There is no correspondingly simple explanation for the apparent stability of these downflows. If the macrocellular pattern were nothing more than a consequence of randomness in the distribution of convection cells, then its coherence time would be comparable with the lifetime of those cells, in sharp contrast with the behavior described above. The lifetime of macrocells is at least 30 times the lifetime of the smaller cells and 8 times greater than the turnover time of the macrocells themselves. Thus, the cause of the long-lived pattern must be *dynamical* and therefore nonlinear. Larger scale organization of small-scale patterns is a generic feature of nonlinear systems, illustrated for instance by experiments on Faraday waves (Kudrolli, Pier, & Gollub 1998).

The horizontal velocity $u_H = (u, v, 0)$ is associated not only with the horizontal divergence field but also with the vertical component of vorticity, $\omega = \partial_x v - \partial_y u$. Although the mean value of ω vanishes when averaged over the entire upper surface, it is in general nonzero when averaged over any subdomain; i.e., the circulation around any patch of fluid is typically finite. Consider now the patch that corresponds to the basin of attraction of a macrocellular downflow (roughly one of the dark areas in Fig. 2): the circulation remains constant, while all the vorticity is swept into the downflow, thereby producing a swirling helical flow with a preferred sense of spin. As expected, we find such downflows with either sense of spin. Moreover, any individual downflow has a sense of spin that persists for a very long time (contrary to what might be expected from a kinematic model). When its spin does change a downflow is particularly fragile and liable to disruption.

In normal unstratified turbulence, slender vortex tubes are relatively short lived (Moffatt, Kida, & Ohkitani 1994). In an unstably stratified layer, buoyancy forces can preserve the swirling downflows. They correspond to Burgers vortices, which are stabilized by convective downflows; conversely, the downflows

are stabilized through advection of vorticity. We therefore conjecture that macrocellular downflows are preserved by the same mechanism as long-lived dust devils and tornados. This process merits further detailed investigation. Our conjecture has two verifiable consequences. Since vertical vorticity is only generated by nonlinear interactions (and not by buoyancy forces), macrocells should manifest themselves only at sufficiently high Rayleigh numbers. Furthermore, the macrocellular pattern should have a finite scale, determined by a balance between the tendency to increase the strength of downflows by increasing the spacing between them and the need to maintain the swirling flow since the net circulation must eventually fall off as the spacing is increased.

Thus far, we have considered only Boussinesq convection, where any pattern at the top must be accompanied by a complementary pattern at the bottom, so we must check that the existence of macrocells does not depend on these assumptions. Fortunately, we have been able to compare the results presented here with behavior found in numerical experiments on nonmagnetic stratified *compressible* convection in a $10 \times 10 \times 1$ box (A. Malagoli & F. Cattaneo 1995, private communication). Moreover, there are indications of related behavior in much more elaborate simulations of photospheric convection (Stein & Nordlund 1998). Since similar macrostructures appear in each case, we can be confident that they do not rely on incompressibility or up-down symmetry. In fact, we would expect strong downflows in a stratified layer to be exceptionally robust.

The structures found in our numerical experiments can therefore be related to those that are observed in the solar photosphere. In our idealized model, the scale of the energy-transporting convection cells is determined by the layer depth; they correspond to granules, whose scale is set by the thickness (of order 500 km) of a strongly superadiabatic “boundary layer” just below the solar surface. The macrocells correspond to mesogranules: both the horizontal velocity and the magnetic field show similar patterns in each case. Thus, mesogranules must owe their origin to collective interactions between granules rather than to stratification or any other cause. Moreover, if our conjecture is correct, these interactions rely critically on concentrating vorticity into vigorous sinking plumes; such slender vortices cannot yet be detected, since correlation tracking is able to resolve only much broader swirling structures. Computations provide no analog for supergranules, which are much larger and penetrate far deeper in the Sun. We presume that their scale is determined by some other mechanism.

We are grateful for helpful comments from Robert Rosner, Thierry Emonet, Keith Moffatt, and Michael Proctor. This work was partially supported by NASA grant NAG 5-4593, by the NASA High Performance Computing and Communication (HPCC) Earth and Space Science Project, and by the UK PPARC.

REFERENCES

- Berger, T. E., Löfdahl, M. G., Shine, R. S., & Title, A. M. 1998, *ApJ*, 495, 973
 Bray, R. J., Loughhead, R. E., & Durrant, C. J. 1984, *The Solar Granulation* (Cambridge: Cambridge Univ. Press)
 Cattaneo, F. 1999, *ApJ*, 515, L39
 Duvall, T. L., & Gizon, L. 2000, *Sol. Phys.*, 192, 177
 Hathaway, D. H., et al. 2000, *Sol. Phys.*, 193, 299
 Kosovichev, A. G., Duvall, T. L., & Scherrer, P. H. 2000, *Sol. Phys.*, 192, 159
 Kudrolli, A., Pier, B., & Gollub, J. P. 1998, *Physica*, 123D, 99
 Lawrence, J. K., Cadavid, A. C., & Ruzmaikin, A. A. 2001, *Sol. Phys.*, 202, 27
 Moffatt, H. K., Kida, S., & Ohkitani, K. 1994, *J. Fluid Mech.*, 259, 241
 Muller, R. H., et al. 1992, *Nature*, 356, 322
 November, L. J., Toomre, J., Gebbie, K. B., & Simon, G. W. 1981, *ApJ*, 245, L123
 Ploner, S. R. O., Solanki, S. K., & Gadun, A. S. 2000, *A&A*, 356, 1050
 Shine, R. S., Simon, G. W., & Hurlburt, N. E. 2000, *Sol. Phys.*, 193, 313
 Simon, G. W., Title, A. M., & Weiss, N. O. 1991, *ApJ*, 375, 775
 ———. 1995, *ApJ*, 442, 886
 Spruit, H. C., Nordlund, Å., & Title, A. M. 1990, *ARA&A*, 28, 263
 Stein, R. F., & Nordlund, Å. 1989, *ApJ*, 342, L95
 ———. 1998, *ApJ*, 499, 914